10

Motion Tracking for Minimally Invasive Robotic Surgery

Martin Groeger, Klaus Arbter and Gerd Hirzinger
Institute of Robotics and Mechatronics, German Aerospace Center
Germany

1. Introduction

Minimally invasive surgery is a modern surgical technique in which the instruments are inserted into the patient through small incisions. An endoscopic camera provides the view to the site of surgery inside the patient. While the patient benefits from strongly reduced tissue traumatisation, the surgeon has to cope with a number of disadvantages. These drawbacks arise from the fact that, in contrast to open surgery, direct contact and view to the field of surgery are lost in minimally invasive scenarios. A sophisticated robotic system can compensate for the increased demands posed to the surgeon and provide assistance for the complicated tasks.

To enable the robotic system to provide particular assistance by partly autonomous tasks e.g. by guiding the surgeon to a preoperatively planned situs or by moving the camera along the changing focus of surgery, the knowledge of intraoperative changes inside the patient becomes important.

Two main types of targets can be identified in endoscopic video images, which are instruments and organs. Depending on these types different strategies for motion tracking become advantageous.

Tracking of image motion from endoscopic video images can be based solely on structure information provided by the object itself or can involve artifical landmarks to aid the tracking process. In the first case, the use of natural landmarks refers to the fact that the genuine structure of the target is used to find reference positions which can be tracked. This can involve intensity or feature based tracking strategies. In the second case of artifical landmarks, markers with a special geometry or colour can be used. This enables particular tracking strategies, making use of the distinctive property of these markers.

This chapter describes different motion tracking strategies used to accomplish the task of motion detection in minimally invasive surgical environments. Two example scenario are provided for which two different motion tracking strategies have been successfully implemented. Both are partly autonomous task scenarios, providing automated camera guidance for laparoscopic surgery and motion compensation of the beating heart.

2. Motion tracking and visual servoing

Visual motion tracking is dealt with here, i.e. tracking of motion from video images. This enables the use of the video endoscope for tracking, as used in minimally invasive surgery

Source: Medical Robotics, Book edited by Vanja Bozovic, ISBN 978-3-902613-18-9, pp.526, I-Tech Education and Publishing, Vienna, Austria

(MIS). Other tracking strategies with special markers and sensors, e.g. optical tracking (e.g. by ARTtrack) or magnetic tracking (e.g. by NDI), which they are hard to be applied in minimally invasive surgery, are not covered.

2.1 Motion tracking

Visual tracking deals with objects of varying positions in a sequence of images. The challenge is to determine the image configuration of the target region of an object as it moves through the field of view of a camera (Hager & Belhumeur, 1998). The task of visual tracking is to solve the temporal correspondence problem, which is to match target regions on successive frames of an image stream.

Tracking involves particular difficulties due to variability in the following parameters:

1. Target pose and deformation: the object can change its position and orientation, and its image can also be deformed, eg. when viewed from different perspectives.
2. Illumination: pixel intensities may change significantly as the scene or parts of it are exposed to different lighting conditions.
3. Partial or full occlusion: the object may vanish from the scene or be partially occluded by other objects.

Tracking strategies Two different tracking strategies can be distinguished: tracking based on image features and tracking of complete regions or patterns in an image. Feature-based tracking requires the extraction of features, which yields robustness against changes of global illumination. But image features may be sparse, which requires additional constraints for the tracking process (Hager & Belhumeur, 1998). While region-based tracking saves the cost of feature extraction, it is burdened with a relatively high computational expense to find the best matching pattern in subsequent images. Direct operation on image intensities requires illumination compensation but has the advantage of using all intensity information available.

Tracking targets The target of tracking, to be detected and followed in a sequence of images, can be a particular image pattern of the object of interest with a distinctive structure. This distinctive structure implies a sufficient contrast in intensity and uniqueness to avoid losing the target in favor of a similar object in the image. Since these criteria may be difficult to fulfill in some environments, it can be advantegeous to aid tracking by the use of so-called *artificial landmarks.* These artificial landmarks are designed with a unique and distinctive structure or colour and are put on the object to be tracked. While this kind of tracking is often referred as being based on artficial landmarks, the other case, in which no additional markers are placed on the object of interest to aid the tracking process can be denoted as tracking based on *natural landmarks.* In this way, natural landmarks refer to prominent parts of the target object in the image. The use of natural landmarks is especially attractive when objects such as organ surfaces are tracked, where artificial landmarks would be difficult to fix. Artificial landmarks often involve a tracking approach, in which image features are extracted which relate to these landmarks. For the case of natural landmarks, the choice between a region- and a feature-based tracking strategy depends on the property of the scene and the target object.

2.2 Tracking of surgical instruments (rigid objects)

In principle, tracking surgical instruments seems much easier than of deformable objects such as organ surfaces, since the tracking targets are rigid. The rigidity property combined

with the fact that the geometry of the objects is known enables the use of a predefined target model. Also, the application of artificial landmarks is much easier, as e.g. colour markers as in (Wei et al., 1997) or (Tonet et al., 2007). However, in the case of surgical instruments with direct contact to human tissue, particular medical requirements such as the biocompatibility and the sterilisability of the artificial markers have to be met (Wintermantel & Ha, 2001).
Most approaches for instrument tracking can be categorised into the two main classes of colour-based strategies and approaches without colour which mainly rely on a geometric model of the instrument.
The use of *colour markers* is particularly attractive, if the environment occupies only a limited range of colour, as is the case for the situs in laparoscopic surgery, which makes the design of a unique colour marker possible (Wei et al., 1997). Similarly, in a more recent publication (Tonet et al., 2007), a colour strip at the distal part of the instrument shaft is used to facilitate segmentation for the localisation of endoscopic instruments. As shown in (Wei et al., 1997) the use of an appropriate colour marker can yield a robust solution for the tracking of surgical instruments.
The approach in (Doignon et al., 2006) does without the aid of artificial markers but uses region-based colour segmentation to distinguish the achromatic surgical instrument from the image background (Doignon et al., 2004) to initiate the search for region seeds. Based on this a special pose algorithm for cylindrically shaped instruments is used to localise the instrument, which can regarded as the second class of model-based approaches.
Doing without the aid of colour information leads to approaches which base their tracking strategy on the geometry of the instrument. These approaches often involve the extraction of edge images of the scene including the instrument, as shown in Fig. 2. As this example shows, this brings along a lot of difficulties to distinguish the instrument from its surroundings. Therefore, these approaches tend to be time consuming and prone to errors, which means that robustness is hard to achieve. A common strategy to detect the instrument without the aid of colour is to use the Hough transform, e.g. in (Voros et al., 2006).

2.3 Tracking of organs (deformable objects)

The particular difficulty with tracking the motion of deformable objects arises from that fact that, in contrast to rigid objects such as surgical instruments, the shape of the object itself changes. Moreover, in the case of organs, an appropriate and precise motion model is hard to estimate and is nonlinear in general (Mclnerney & Terzopoulos, 1996). Tracking deformable objects often involves the estimation of deformation in a particular image area, e.g. to extract face motions (Black & Yacoob, 1995) or to track surfaces in volume data sets of the beating heart (Bardinet et al., 1996; Mclnerney & Terzopoulos, 1995).
However, if the temporal resolution of the image stream is sufficiently high, such that changes between two subsequent images are small, approximating the deformation by a rigid motion model (consisting of e.g. translation! and rotation) is often sufficient, as investigated in (Shi & Tomasi, 1994). This enables local structures of deformable objects to be tracked efficiently.
Fixing artificial markers to deformable objects is difficult, in particular in the case of organ surfaces. Therefore, tracking approaches based on natural landmarks are advantageous, which often involve a region-based strategy.
A region-based approach designed to enable robust motion tracking of the beating heart surface using natural landmarks (Groger et al., 2002) is described in more detail below in a scenario to compensate motion of the beating heart by a robotic system (5).

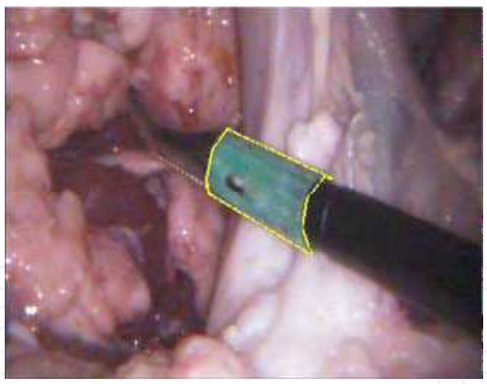

Figure 1. Laparoscopic instrument with colour marker (DLR)

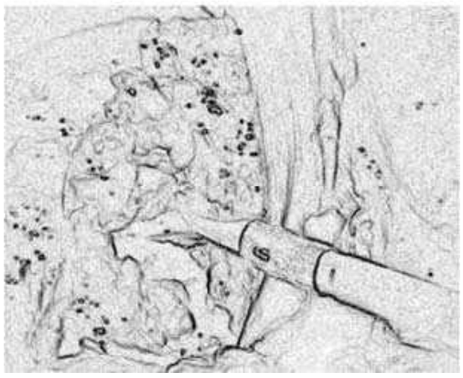

Figure 2. Edge image of laparoscopic instrument with colour marker

2.4 Visual servoing

"Visual servoing" in robotics denotes the control of an end effector in a control loop closed by imaging sensors. This requires the estimation and tracking of position and orientation of objects in the three-dimensional space, based on camera images (Corke, 1993; Hutchinson et al., 1996). Visual servoing involves the use of methods from realtime image processing, from visual tracking, and from robot control theory.

Many existing systems for visual servoing are based on artifical landmarks, which are mounted to the object of interest. However, this often increases the effort to set up the system or is hard to achieve, as e.g. with tracking of deformable objects such as organs. A region-based approach, which does not need any particular kind landmarks is described in (Hager & Belhumeur, 1998). This tracking system is successfully applied in a system for robust hand-eye coordination based on images of a stereo camera (Hager, 1997).

The use of stereo imaging from a stereo endoscope enables to estimate the three-dimensional position of the target, which is necessary for visual servoing tasks in 3D environments.

Two visual servoing scenarios for minimally invasive surgery are presented below. The automated la-paroscope guidance system enables a robot to automatically adjust the camera position to the current field of surgery (section 4). It is based on tracking a rigid object (surgical instrument) with aid of an artificial landmark (colour marker) mounted on it. The second scenario of motion compensation of the beating heart applies a region-based strategy with natural landmarks to track the motion of a deformable surface (the heart). Robust

tracking of the heart, combined with a sophisticated robotic system enables to compensate the motion of the beating heart during surgery (section 5).

3. Minimally invasive robotic surgery

3.1 Minimally invasive surgery

Minimally invasive surgery only requires small incisions into the patient body. These incisions are used too introduce endoscopic instruments into the patient body, and also to insert an endoscopic camera, which provides a view of the site of surgery surgery inside the patient. In contrast to open surgery, minimally invasive surgery minimises trauma for the patient, decreases the loss of blood, speeds up patient convalescence, and reduces the time of the patient in the hospital.

While minimally invasive surgery brings along clear benefits for the patient, the surgeon is faces strongly increased demands, especially since direct contact to the field of surgery is lost. A sophisticated robotic system can compensate for the increased demands posed to the surgeon and provide assistance for the complicated tasks.

3.2 Robotic support for invasive robotic surgery

Surgical robots have been developed for a variety of specific applications, as summarised in (Taylor & Stoianovici, 2003). Most early first uses of robots in surgery occurred in neurosurgery (Y. S. Kwoh & et al., 1988), but the field soon expanded to other disciplines such as orthopaedics (Taylor et al., 1989,1994; Kazanzides et al., 1995) and laparoscopy (Sackier & Wang, 1996).

The use of robots allows to increase the accuracy of surgical interventions, as shown by early robotic systems in neurosurgery (Y. S. Kwoh & et al., 1988) and orthopaedics (Mittelstadt et al., 1996; Bargar et al., 1998). In minimally invasive surgery the drawbacks caused by loss of direct access to the field of surgery can be compensated by the aid of robotic systems, combined with techniques from the field of telepresence. Cartesian central, e.g., overcomes the the so-called "chopstick effect" when performing surgery through small incisions (Ortmaier & Hirzinger, 2000). Combined with increased dexterity of specially designed instruments (Rubier et al., 2005) this enables the surgeon to lead the instruments similar to in open surgery and to regain the dexterity as in open surgery. Force feedback (Preusche et al., 2001) together with specially designed sensorised instruments (Kubler et al., 2005) enables the surgeon to feel forces occurring at the tip of the instrument during surgery. Moreover, the use of stereo endoscopes enable a three-dimensional view to the field of surgery and as in open surgery. Different techniques of 3D display devices, such as head-mounted displays (HMDs) or a stereo console as in the daVinci system (Guthart & Salisbury, 2000).

The combination of preoperative planing with the surgical intervention enables intra operative support for the surgeon by medical robots, such as the guidance of instruments (Ortmaier et al., 2001).

3.3 Visual servoing for robots in medicine

Visual servoing closes the control loop between imaging sensors and robot control. It enables to perform partly autonomous tasks, depending on the current situation in the field of surgery.

Examples for autonomous robot functions are tasks to supervise the working room or the automated guidance of the camera in laparoscopy (Wei et al., 1997). Different scenarios, in particular from soft tissue surgery are the guidance of the robot end effector to particular positions, in relation to given tissue structure, e.g. to hold a lighting source or tissue parts, or the autonomous movement of the robot end effector to particular positions, as e.g. in liver biopsy.
Moreover, one can think of compensating the motions of organs, such that the relative configuration and distance between instrument and organ surface remains constant. Thus, the organ is stabilised virtually. In this case, however, it is also necessary to integrate the video image provided to the surgery into the motion compensation procedure and to maintain overall consistence of motion compensation.

Figure 3. ZEUS robotic system by Computer Motion Inc

Figure 4. DaVinci robotic system by Intuitive Surgical Inc

3.4 Robotic systems for minimally invasive surgery

Many robotic systems that have been applied to surgery are based on industrial robots, as e.g. the *Robodoc* system for for hip surgery (Kazanzides et al., 1995; Taylor et al., 1994; Bargar et al., 1998), and are therefore large, heavy and hardly flexible. Other robotic systems, specially desgined to be applied for surgery, such as the *ZEUS* system ((Sackier & Wang,

1996), Fig. 3) by Computer Motion Inc. (Goleta, CA, USA; now: Intuitive Surgical Inc.) and the *daVinci* system ((Guthart & Salisbury, 2000), Fig. 4) by Intuitive Surgical Inc. (Cupertino, CA, USA) are much more flexible and light-weight. These systems are sufficient for laparoscopic assistance tasks such as the automated guidance of a laparoscope to provide the surgeon with a view of operating field. This is shown in the first example scenario below (section 4).
These robotic systems, however, lack the high degree of precision needed for orthopaedic surgery and additionally the high dynamics required for following the motion of the beating heart (section 5). The newly developed KineMedic surgical robot was specially designed to account for these increased demands, providing both light-weight and flexibility and the required high dynamics and precision.
The design of the KineMedic robot is based on the method of soft robotics pursued at the Institute of Robotics and Mechatronics, DLR, which leads to robotic systems such as the DLR light-weight robot (Hirzinger et al., 2001), which are light-weight, flexible and modular, and still maintain a high degree of dynamics and accuracy. Based on these techniques, the newly designed KineMedic robot has been developed as a joint partnership of DLR and BrainLab AG (Heimstetten, Germany), focussing on the demands of surgery (Ortmaier et al., 2006).

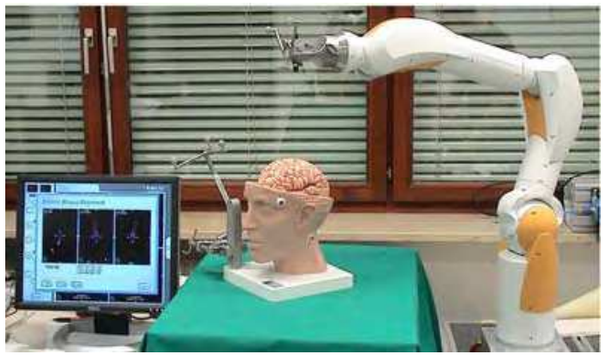

Figure 5. DLR-KineMedic medical robot arm

The KineMedic surgical robot (see prototype in Fig. 5) consists of sophisticated light-weight robotic arms, which reach a payload of 3 kg at a dead weight of only 10 kg. The redundant design of the robotic arm with seven joints enables, using null-space motion, to reconfigure the position of the robot, while the position and orientation of the instrument remains in the same position. With force-torque sensors, implemented in addition to the redundant design of the robot, the reconfiguration of the position can be performed in an intuitive way by touching and pushing the robot into the desired direction. Furthermore, the redundancy can be used to implement an arm control system which avoids collisions, which enables a more flexible setup in the operating room. Since the robot is built in light-weight design, it can be mounted or removed easily by a surgeon or nurse during a surgical intervention. This reduces mounting times in the operating room. For minimally invasive surgery usually two of these robot arms are used to manipulate surgical instruments, while a third arm moves the endoscope. An example of such a scenario is is presented in Fig. 6. The KineMedic robot arm is controlled at a rate of 3 Hz and has a high relative positioning accuracy. This way, the robot provides the dynamics required for following the motion of the beating heart.
The new KineMedic robot shows significant improvements on the medical robots avaible so far and enables highly demanding scenarios such as compensation the motion of the beating heart.

4. Automated laparoscope guidance

In laparoscopic surgery, the surgeon no longer has direct visual control of the operation area, and a camera assistant who maneuvers the laparoscope is necessary. Problems of cooperation between the two individuals naturally arise, and a robotic assistant which automatically controls the laparoscope can offer a highly reliable alternative to this situation. In this section a autonomous laparoscopic guidance system for laparoscopic surgery is described, developed at the DLR's robotics lab and thoroughly tested at MRIC (Department of Surgery at the Klinikum rechts der Isar (MRIC) of the Technical University of Munich) (Wei et al., 1997; Omote et al., 1999).
A robot holds the laparoscope and directs it to the operative field by means of image processing techniques. The method is based on colour coded instruments. The system originally operated at a maximum rate of 17 Hz for stereo-laparoscopes and 34 Hz for mono-laparoscopes (Wei et al., 1997). It now easily runs on a standard PC in realtime for stereo-laparoscopic images delivered at a framerate of 25 Hz. For mono-laparoscopes, tracking only in lateral directions (left/right and up/down) is enabled, but for stereo-laparoscopes tracking in the longitudinal direction (in/out), too.

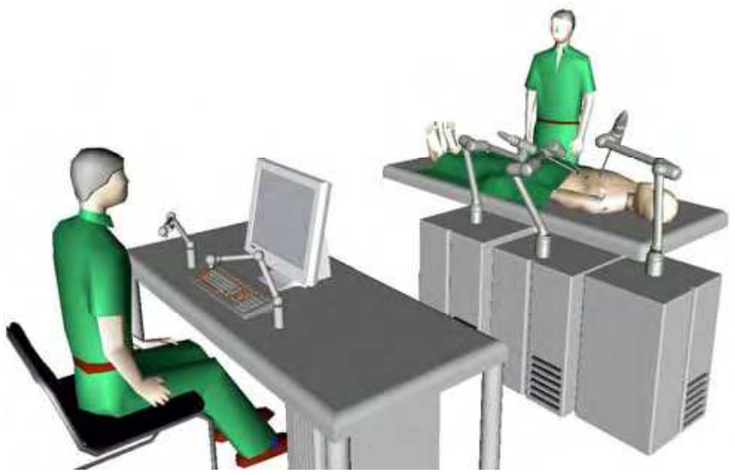

Figure 6. DLR scenario for minimally invasive robotic surgery

During the initial period of clinical evaluation 20 laparoscopic cholecystectomies have been performed and compared with those using human camera control. The longer set-up time was finally compensated by a shorter operation time. The frequency of camera correction caused by the surgeon as well as the frequency of lens cleaning was much less than with human control. The smoothness of motion was much better with the robot than with human assistants. Subjective assessments by the surgeon revealed that the robot performed better than the human assistant in a significant majority of cases.

4.1 Introduction

Laparoscopic surgery is minimally invasive, which offers the advantages of reduced pain, shorter hospital stay, and quicker convalescence for the patients. Unlike open surgery, laparoscopic surgery needs only several small incisions in the abdominal wall to introduce instruments such as scalpels, scissors, and a laparoscopic camera, such that the surgeon can operate by just looking at the camera images displayed on a monitor screen. While in open

surgery vision and action are centered on the surgeon, he loses direct visual control in laparoscopic surgery. Another person, the camera assistant, has to point the laparoscope to the desired field of vision. The surgeon has to give instructions as to where the scope should be focused, and the camera assistant has to follow them. This naturally gives rise to problems of cooperation between the surgeon and the camera assistant. A certain amount of the assistant's experience and a mutual surgeon-assistant understanding are necessary, but usually difficult to obtain. The surgeon frequently has to give the commands to move the laparoscope onto the desired area of view. This gives him an additional task, detracting his attention from his main area of concentration. The laparoscopic image may become unstable in a long operation due to fatigue of the camera assistant.

To deal with these problems, several robotic assistance systems have been developed (Hurteau et al., 1994), (Taylor et al., 1995), (Sackier & Wang, 1996) to provide more precise positioning and stable images. For a more comprehensive review of robotic systems in other surgeries see (Taylor et al., 1994), (Troccaz, 1994), (Moran, 1993), and (Taylor & Stoianovici, 2003). Investigations indicate that the use of robots in surgery reduces personnel costs while almost maintaining the same operation time (Turner, 1995). A surgical robot may be controlled either by an assistant using a remote controller or by the surgeon himself using a foot pedal (Computer Motion Inc., 1994). Voice control seemed to be another attractive alternative, as it was available with the AESOP3000 medical robot arm (by Computer Motion Inc., Goleta CA, USA).

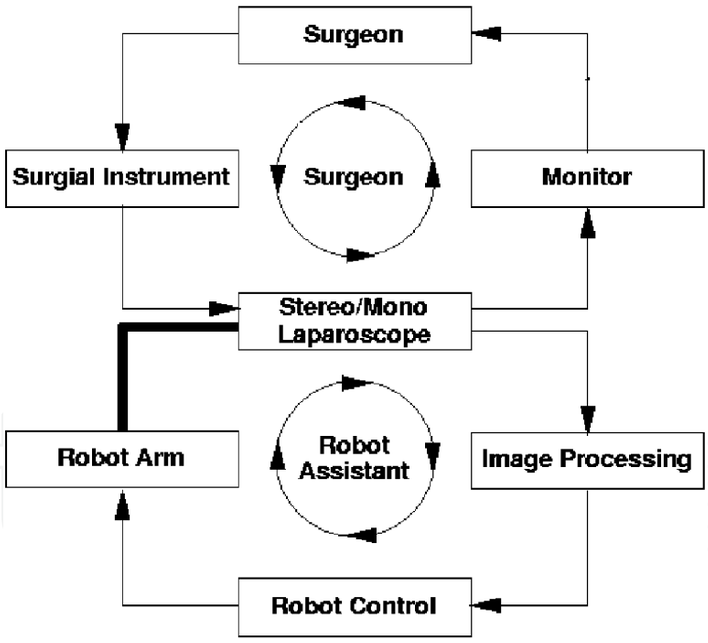

Figure 7. The structure of image-based robot-assisted minimally invasive surgery

To avoid the need for another assistant and to free the surgeon from the control task, an autonomous system that automatically servoes the laparoscope is highly desirable. The basic structure of an image based system is shown in Fig. 7. The surgeon handles the surgical instruments dependent on his observations on a monitor where the laparoscopic image is displayed, as usual in minimally invasive surgery. But instead of a human, the laparoscope is held by a robot arm which is controlled via an image processing system in order to track

the surgical instrument smoothly. The use of the laparoscope as a sensor for the tracking system sounds attractive, because no extra sensor is needed, but it's hard to obtain reliable control signals under realistic clinical conditions and safety requirements. The dominant problems for image processing are ambiguous image structures, occlusions by blood, organs or other instruments, smoke caused by electro-dissection, and the need of (quasi-)real-time image processing. With respect to the slow robot motions during a surgery, an image processing rate of about ten frames per second (10 Hz) is considered to be enough, but is a lower limit to maintain the impression of smooth motion.

Several researchers have tried to use image processing techniques to track the instrument such that it is always centered in the visual image. Lee, *et al,* (Lee et al., 1994) used the colour signatures of the image to segment the instrument. Since the instrument and background often possess the same colour components, much post-processing, such as shape analysis, has to be done to remove false segmentations and to extract the position of the instrument in the image. No real-time implementation was reported in, (Lee et al., 1994), and it is not known whether the complexities of their shape analysis may allow implementations applicable to surgical operations. Casals, *et al.* (Casals et al., 1995), used patterned marks on the instrument to facilitate image segmentation by searching for the presumed structure in the contour image. The method was reported to operate at a rate of 5 Hz for a mono-laparoscope using customised image processing hardware. Since both the methods in (Lee et al., 1994) and (Casals et al., 1995) rely on the existence of a preassumed shape or structure, they may fail if the camera is to near to the instrument, or if the instrument is partially occluded by organs or contaminated by blood. In both cases, the preassumed shape may not be present. Taylor, *et al.* (Taylor et al., 1995), used multi-resolution image correlation to track an anatomical structure specified by the surgeon with an instrument-mounted joystick that controlled a cursor on the video display. A problem with this method might be that the anatomical structure deforms and may completely change its appearance due to manipulation of the organs.

We propose a visual laparoscope-tracking method which is simple and robust (Arbter & Wei, 1996), (Arbter & Wei, 1998). The laparoscope may be a mono-laparoscope or stereo-laparoscope. A mono-laparoscope enables the robot to track the instrument in the lateral directions left/right and up/down, while a stereo-laparoscope provides depth information and can be used to control the distance between the tip of the laparoscope and the instrument. Due to the multiplicity of problems with shape analysis, we do not check for the presence of any particular shape or structure. Instead, we use colour information alone for instrument segmentation. The non-uniqueness of the instrument colour inspires us to use an artificial colour-marker to distinguish the instrument (Fig. 12a). To mark the instrument, the colour distribution of typical laparoscopic images is analysed and a colour is chosen which does not appear in the operational field (the abdomen here). With colour image segmentation, the marker can be correctly located in the image and used to control the robot motion. Thus, even if only a very small part of the marker is visible, reliable data can still be obtained for robot control.

To build up an experimental system, only commercially available hardware was used, with the instruments from Bausch Inc., Munich, Germany, the stereo-laparoscope system from Laser Optic Systems Inc., Mainz, Germany, the AESOP 1000 robot from Computer Motion, Goleta, USA, the MaxVideo 200 image processing system from Datacube Inc., USA, and a M68040/25MHz host-CPU from Motorola Inc., USA. The coloured markers have been

placed on the instruments by the manufacturer. The electronic components are integrated into an electronic radiation protecting cabinet being mobile and used as transportation car for the robot arm, too.

Figure 8. DLR automated camera guidance scenario with AESOP robot

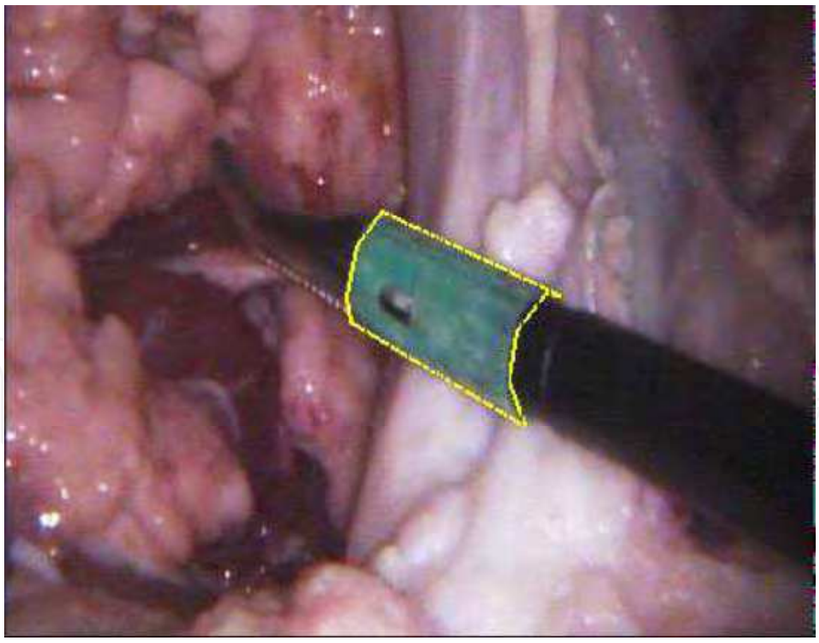

Figure 9. Laparoscopic instrument with colour marker (DLR)

For the initial period of clinical tests the system was evaluated in 20 laparoscopic cholecystectomies and compared with those using human camera control.

In the following, the image processing module, the robot controller module, and the experimental results are presented.

4.2 Image Processing

Figure 10 shows a block diagram of the image processing module. The inputs are the analog video *RGB-signals,* either from the CCD-camera pair of the stereo-laparoscope, or from only one CCD-camera of a mono-laparoscope. The inputs are **time multiplexed** at the video frame rate of 25 Hz (CCIR) in order to spend only one image processing hardware to process the stereo-images. Then the analog signals are converted into digital *RGB-signals* of 8 bits each. The *RGB* data stream is **converted** to the *HSV* format (Hue, Saturation, Value) for reasons explained below. The **classifier** separates two classes of pixels, those having the colour of the marker and those not. The result is a binary image containing the object separated from the background. The classifier is the kernel of the image processing module and will be explained in detail below. The **localiser** computes the bounding box and the centre of gravity of the object pixels as well as their number (size of region). The bounding box is then used to define the region of interest (ROI) for segmentation of the next frame. The use of an ROI speeds up the segmentation procedure and improves the robustness against misclassification. Figure 11 shows a stereo-laparoscopic image (of an experimental environment) superimposed by the centres of gravity and bounding boxes of the segmented marker.

4.2.1 Colour representation

A colour can be represented by its red, green, and blue components *(RGB)*. In digital 8bit-images, the *RGB* values are between 0 and 255. Thus colours can be represented by the points within the *RGB* cube of size 256 x 256 x 256. The *RGB* colour space can be transformed to another colour space, the *HSV* colour space (Hue, Saturation, Value) where only two components *H* and *S* are directly related to the intrinsic colour and the remaining component *V* to the intensity. Different *RGB-to-HSV* transformations are known in video technology and computer graphics. We have used the following one (Foley et al., 1990):

$$r = R/R_{\max}, \qquad g = G/G_{\max}, \qquad b = B/B_{\max} \tag{1}$$

$$\min = \text{Minimum}\{r, g, b\} \tag{2}$$

$$\max = \text{Maximum}\{r, g, b\} \tag{3}$$

$$\Delta = \max - \min \tag{4}$$

$$H = \begin{cases} 60^o \ (g-b)/\Delta & : \max = r \\ 60^o \ (b-r)/\Delta + 120^o & : \max = g \\ 60^o \ (r-g)/\Delta + 240^o & : \max = b \end{cases} \tag{5}$$

$$S = (\max - \min)/\Delta \tag{6}$$

$$V = \max \tag{7}$$

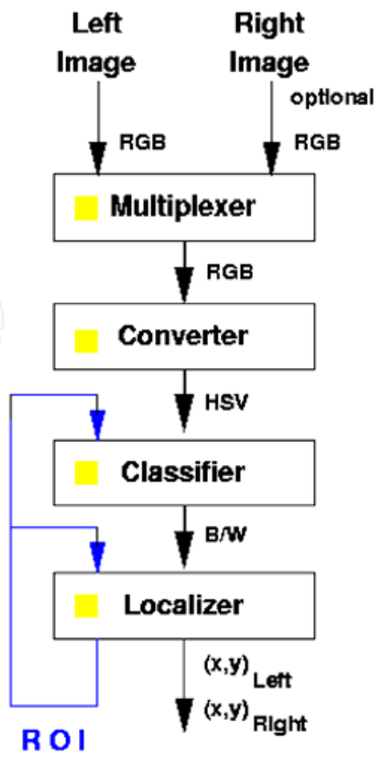

Figure 10. Structure of the image processing module

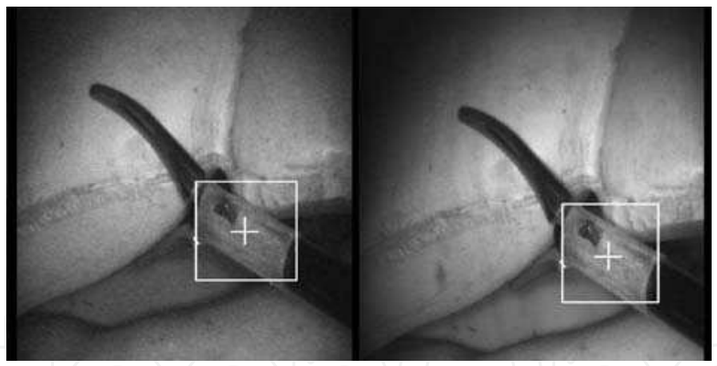

Figure 11. A stereo laparoscopic image superimposed by the centres of gravity and bounding boxes of the segmented marker

In laparoscopic surgery, we would like the image segmentation results to be insensitive to the strength of illumination. The *H* and *S* are insensitive to the strength of illumination, if only one light source, having a certain colour temperature, is used, as is the case in laparoscopy. One advantage of the *H S* colour space is its 2-dimensionality in contrast to the 3-dimensionality of the *RGB* colour space, so that the colour signature of a colour image can be directly analyzed in the *H S* plane. Figure 12d shows a colour space of the *H S* representation, filled with the corresponding colour, where the brightness is set to 255. In this coordinate system, the *H* value is defined as the angle from the axis of red colour, and the *S* value (normalised to the range of zero to one) is the length from the origin at the centre.

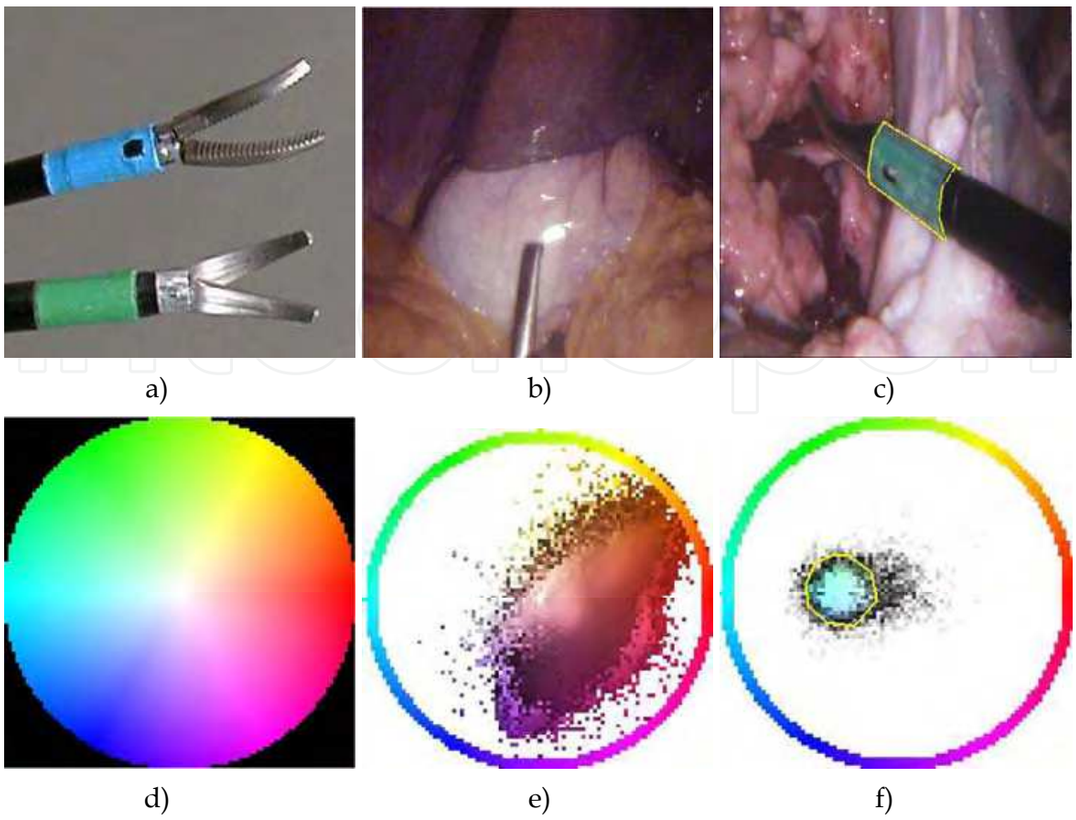

Figure 12. (a) Distal ends of colour coded minimally invasive surgical instruments (b) A typical laparoscopic image (c) Marker image with polygonal boundary (d) HS colour space (e) Colour Histogram of the abdominal scene (f) Colour histogram of the marker superimposed by the polygonal classifier boundary (cluster-polygon)

4.2.2 Marker colour selection

To choose the colour to be brought onto the instrument, we analyzed the colour components of real laparoscopic images recorded on a video tape. Typical abdominal images containing variations of colours are manually selected. Figure 12b shows one of the 17 images used in our colour analysis. An array of counters in a quantised *HS* domain is set to zero at the start. Then, for each pixel in the images, we compute its *HS* values and increment the counter by 1 at the corresponding *HS* position. The result is a 3-D histogram, which indicates the frequency of occurrence of all the colours in the analyzed images. To give an intuitive perception of the histogram, we display it in a colour image format, with the brightness (V) set proportional to the frequency of occurrence and the *HS* values equal to the *HS* coordinates in the *HS* plane. Figure 12e shows such a histogram, where the ring near the image boundary is used to help perceive the overall colour distribution. The crescent bright region within the ring represents the colours that do not appear in the images and can thus be used as the colour to be marked on the instrument. For the marked colour to be optimally distinguishable from those present in the image, the colours near the cyan are preferred, as can be seen in Fig. 12e. After the admissible colours have been determined, we have to consider the material which carries the desired colour, its commercial availability, and its

biocompatibility. On account of these factors, we have used a near-cyan plastic ring, as shown in Fig. 12c.

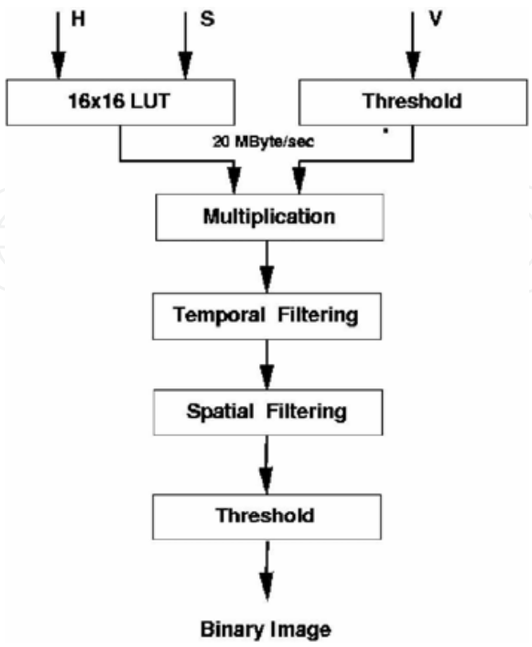

Figure 13. Classifier structure

4.2.3 Colour training selection

Due to the colour distortion through laparoscopes, we have to locate the actual position of the chosen colour in the *H S* plane. We select a set of typical images showing the marker in different situations, e.g., near, far, slanted, or orthogonal to the view direction, and calculate the colour histograms from the marker regions only. We first manually outline the marked instrument in the image with a polygonal boundary as shown in Fig. 12c. Then, the pixels within the polygon are used to compute the colour distribution in the *H S* plane. Figure 12f shows the colour cluster of the marker.

To represent the corresponding individual marker colour space, we again use a polygonal approximation of the cluster boundary Fig. 12f. By backprojection of the enclosed colours to the original training set and by modifying the boundary, we iteratively minimise the number of misclassified background pixels by simultaneously maximizing the number of correctly classified marker pixels. We repeat this procedure for all the images out of the training set, resulting in a set of colour regions. The union of the individual regions represent the marker colour space, and we call its border cluster-polygon. The above process is called colour training, and is of the type of supervised learning.

4.2.4 Colour classifier

The kernel of the colour classifier (Fig. 13) is a 16-bit look-up table (LUT). This LUT is the implementation of the region beeing bounded by the cluster-polygon. Its input is a data stream of 16-bit *HS* values, which are formed by concatenating the 8-bit *H* and 8-bit *S* values. Its output is binary and indicates whether the input value falls within the cluster-polygon or not. Low intensity pixels do not provide reliable *H S* values and are themselves of no interest. Thus,

pixels beeing classified as marker pixels, but having an intensity below a certain threshold are reset to zero (background) by multiplication of the LUT output with the thresholded intensity *V*. This step of postprocessing would not be necessary, if *RGB* values would be used as input. But the use of a 16-bit LUT requires to reduce the resolution to 5 bits for each *RGB* component. This is an other reason, why we preferred the *HSV* colour space. Fig. 14 shows the initial segmentation of Fig. 12c using the cluster-polygon of Fig. 12f. It can be seen from Fig. 14 that most of the marker pixels are correctly classified, yet some of them and a few background pixels are misclassified. Misclassification of marker pixels is much less critical than of background pixels and can be accepted up to a considerable amount since no shape analysis is used. Although we could avoid false segmentations of background pixels by choosing a smaller cluster-polygon, but this would also eliminate too many pixels belonging to the marker. The classification errors tend to be scattered, as well in the space as in the time domain. Furthermore, the space-frequency bandwidth of the marker region is much lower than the bandwidth of the scattered errors. Therefore the inital segmentation can efficiently be improved by spatio-temporal lowpass postprocessing. We add successive binary frames (time-domain lowpass) and convolve the result with a 7 x 7 box operator (space-domain lowpass, local 7 x 7average). By thresholding the low-pass filtered image, not only misclassified background pixels are removed, but also misclassified marker pixels are recovered, thus the marker region becomes more compact, as shown in Fig. 15. A special colour classifier design tool (CCDT) has been developed, which allows for an easy design of a colour classifier (Arbter & Kish, 2004).

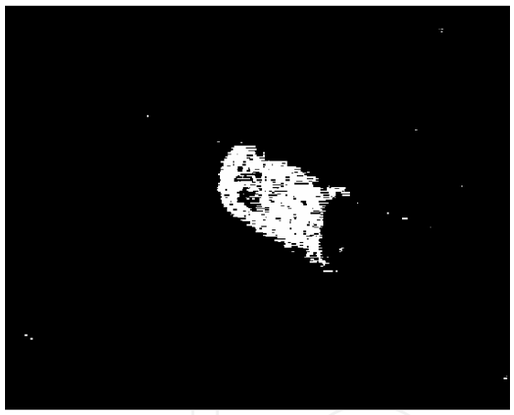

Figure 14. Colour segmented marker

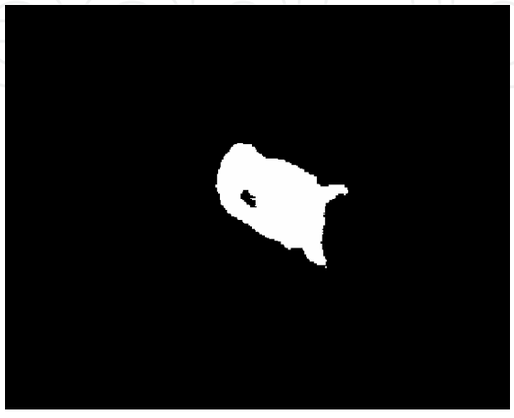

Figure 15. Postfiltered segmentation result

4.3 Robot Controller

The task of the controller is to bring the actual image of the instrument to a desired location at the monitor screen by smoothly moving the robot according to the incoming signals from the image processing system. The desired location is either prestored, or it can be redefined on-line by moving the instrument to the desired monitor position, while the tracking mode is switched off. In the second case the image processing module extracts the actual location values and stores them as reference coordinate values for the future.

As input to the robot controller, we have used the centers of gravity as well as the corners of the bounding boxes. We made the experience that corners are much more reliable in most cases than centres of gravity, especially in the case where the marker is partially occluded.

Since the AESOP 1000 robot system (Computer Motion Inc., 1994) provides direct motion control in the image plane, no user-involvement in the robotic kinematics is necessary. The commands **MoveLeft ()** and **MoveRight ()** specify robot motions such that the laparoscopic image moves to the left and right of the human eyes looking at the monitor image; that is, they specify the *x*-direction motion in the image coordinate system. Similarly, **MoveUp ()** and **MoveDown ()** control the motion in the *y*-direction in the image plane. Motions orthogonal to the image plane (longitudinal *z*-direction motions) are specified by the **Zoomln ()** and **ZoomOut ()** commands.

Suppose (x_L^0, y_L^0) and (x_R^0, y_R^0) are the reference coordinate values in the left and right images, respectively. Suppose (x_L, y_L) and (x_R, y_R) are the current coordinate values of the colour marker location in the left and right camera images, respectively. Then, we determine the 3D-speed command of the robot motion as follows:

$$\begin{aligned} v_x &= \alpha[(x_L - x_L^0) + (x_R - x_R^0)] \\ v_y &= \alpha[(y_L - y_L^0) + (y_R - y_R^0)] \\ v_z &= \beta[\sqrt{(x_L - x_R)^2 + (y_L - y_R)^2} - \\ &\quad \sqrt{(x_L^0 - x_R^0)^2 + (y_L^0 - y_R^0)^2}]. \end{aligned}$$

The equations reduce in the case of mono-laparoscope to:

$$v_x = \alpha(x - x^0), \qquad v_y = \alpha(y - y^0).$$

This intermediate commands are then converted to the specific **Move . . . (speed)** commands by separating magnitudes and signs for speed and direction.

With this control law the closed loop system has approximately a first order low-pass transfer function. The bandwidth (dynamics) depends on the values *a* for lateral motions and *0* for longitudinal motions, respectively, and may easily be adapted to the surgeon's needs. The system follows asymptotically slow instrument motions, as they occur if the surgeon changes the operational field, but damps fast motions, as they occur if the surgeon treats the tissue. This behavior provides the surgeon with smoothly moving images in the first case and with quasi-stable images in the second case, as is desired.

4.4 Robustness

Safety is of the highest priority in surgery. The correct segmentation of instruments is crucial for correct visual guidance. A problem particular to laparoscope images is that the received light by the narrow lens system is usually very weak, so that the CCD signal (including noise) has to be highly amplified. For this reason, the signal-to-noise ratio is considerably lower than that of a standard CCD-camera. In our system, the high rate of correct colour segmentation in the presence of noise is attributed to the use of spatio-temporal low-pass filtering.

Occlusion of instruments occurs very often during surgical operations. It can be caused either by another instrument or by organs. As far as the lateral motion control is concerned, partial occlusion is by no means a hindrance, since no precise motion control is necessary. Besides, partial occlusion does not affect image-tracking either, because no shape analysis is used in the tracking. In the case of complete occlusion, the colour code can be re-allocated, when it re-appears, at almost the same speed as it is tracked. It may happen that in few critical situations, e.g., when the colour code is too far away from the laparoscope, either the left or the right colour code is not fully segmented due to uneven illuminations. In such a case, the computed disparity provides wrong information about depth. In our sytem the bounding boxes are permanently checked with respect to their difference in size. If this difference is greater than a threshold, e.g., 40 pixels, the z -direction motion control is blocked.
Another characteristic of laparoscope images is that saturation may occur caused by too intensive illumination, or by specular reflections at moist organ surfaces. The highly saturated part in the image is white in colour. When saturation occurs on the instrument, e.g., when the instrument is placed too near to the laparoscope, the saturated part loses its original colour of the colour-code. But since the instrument is cylindric in shape, i.e., the surface normals vary in a wide range, the probability of complete saturation of the colour-marker is extremely low. Particulary those regions where the normals are oriented towards the light source tend to be saturated. In this sense, saturation is similar to partial occlusion.
Furthermore, due to the use of the region of interest (ROI) in the classifier, the segmentation result will not be disturbed by any events outside ROI. For instance, the visual attention of the robot will not be redirected toward the image boundary when a second instrument appears there. Also, the reaction time of the robot assures image stability. Any quick movement of the instrument, e.g., due to instrument change, will not cause the robot to follow. Still, as the statistics processor provides the number of colour-marker pixels, we use it as another security check. If the pixel number is less than a threshold, e.g., 50, then a decision is made that no object is reliably segmentable, and the robot remains stationary.

4.5 Performance characteristics

The image processing system MaxVideo is a pipeline processor working at 20 MHz. Its image processing components such as colour transformation, colour classification (LUT), temporal filtering, spatial filtering,
localisation, and bounding box extraction are working in parallel. The result is transferred via VME-Bus to the host CPU where the robot controller, safety check, and the interface to the AESOP robot are implemented. The system works asynchronously at a maximum rate of 34 Hz for mono-images and of 17 Hz for stereo-images when the region of interest has been found, and at a minimum rate of 15 Hz for stereo-images, when the region of interest is the whole image of 512x512 pixels for each of the two images. The rate might be doubled by using double buffering technique, in which image acquisition and image processing work in parallel, too. But this is not necessary for our task.
A recent implementation of the system runs on a standard PC (Intel Pentium 4,2.6 GHz Xeon) in realtime for stereo-laparoscopic images delivered at a framerate of 25 Hz.

4.6 Experiments and evaluation

The system has first been tested in a dummy abdomen used for surgical training. Artificial (plastic) organs as well as as real organs (of pigs) have been used. During this phase the

surgeons learned to use the system. Furthermore system parameters, as dynamic behavior, have been tuned to the surgeons needs, and the classifier could have been refined (LUT, thresholds).

The system was then tested on pigs at the Klinikum rechts der Isar, Technical University of Munich. Of particular importance where the tests of the system performance under the following typical disturbances:

- partial occlusion by organs or another instrument,
- staining by blood or gall juice,
- rinsing fluid,
- smoke caused by electro-dissection and coagulation.

The visual guidance in the cavity of the pigs was very successful and there were no cases in which the robot was wrongly guided.

During the initial period of clinical evaluation, that followed, 20 laparoscopic cholecystectomies on humans have been performed and compared to 58 laparascopic cholecystectomies under human assistance. The evaluation included the parameters set up time, operation time, frequency of lens cleaning, frequency of camera correction, and incidence of intraoperative complications. Student's test was used for the statistical analysis and values of $p < 0.05$ were considered to be significant. After laparoscopic surgery using the robotic system, the surgeon completed a questionnaire to asses subjectively the performance of the robotic system compares to a human assistant.

The set up time for the robot system was defined as the interval from the point at which the robot arm was attached to the side of the operation table until laparoscopy started. This time period was compared to that needed without the robot, namely the interval between connection of the sterilised tubes to the equipment and the initial insertion of the laparoscope into the abdominal cavity. The surgical time was defined as the interval from the beginning of the cholecystectomy and the moment when the laparoscope was finally extracted. Contamination of the optical lens caused by contact with internal organs or intraperitoneal fluid is very bothersome because in this case the laparoscope has to be extracted and to be cleaned. The frequency [events/hour] of lens cleaning is therefore an important assessment parameter in laparoscopic procedures as well as the frequency of camera corrections by the surgeon. With the robotic system those corrections are necessary if the reaches the border of his working space. If the human assistant misguides the laparoscope then the surgeon intervents sometimes manually but mostly by a verbal instruction to the assistant.

The mean set up time for the robot system (21 minutes) was considerably longer than that without the robot (9 minutes). But, before the system was integrated into the mobile cabinet, the setup time was up to 55 minutes. With the integrated system the setup time was reduced to around 15 minutes.

The surgical time using the robot was between 35 and 70 minutes. The mean value of 54 minutes was 6 minutes shorter than with human assistance, although the difference between the two was not statistically significant ($p>0.05$).

The mean frequency of interruptions for lens cleaning was only I/hour compared to 6.8/hour with the human assistance ($p<0.0001$). This improvement is a consequence of the utilization of a stereo laparoscope within an automatic control loop which maintains the distance between the lens and the marker, and which stops longitudinal motion if the marker becomes inivisibile in at least one image of the stereo image pair.

Similarly the mean frequency of interventions of the surgeon for correcting the position/orientation of the camera decreased from 15.3/hour with human assistance to 2.2/hour with the robotic system. This improvement is basically the consequence of the automatic guidance concept.

	Units	Robot Assistance n=20	Human Assistance n=58	Statistical Significance P
Setup time	minutes	21 [10-55]	9	<0.0001
Operation time	minutes	54 [35-70]	60	>0.05
Lens cleaning	events/h	1.0	6.8	< 0.0001
Camera	events/h	2.2	15.3	< 0.0001
Complications	technical anatomical	2 1		

Table 1. Clinical evaluation results

The procedures were successfully completed in 17 cases with the robot camera assistant, but were interrupted in the 3 remaining cases. In two of the latter cases robot camera control had to be changed to human camera control, and the remaining one case was converted to open surgery because of anatomical reasons. In the first case that was transferred to human camera control the reason was insufficient white balancing of the laparoscope. In the second case, there was a problem in positioning of the robotic arm, which disturbed the free movement of the surgeon. The troubles that arose in these two cases were avoided in future operations.
Subjective assessment by the surgeon revealed that the robot camera control performed worse in 12.5% , equal in 12.5%, and better in 71% of the cases. This statistical result is dominated by the two cases mentioned above, where the procedure was interrupted due to technical reasons, which are not relevant in the future. Furthermore the smoothness of motion was emphasised as an important improvement, supporting the surgeons concentration. For more details see (Ungeheuer et al., 1997) and (Omote et al., 1999).

4.7 Conclusion

We have described an autonomous, real-time visual guidance system for laparoscopic surgery. The system is based on commercially available hardware components. We proposed to use colour marking on the instrument for simple and reliable segmentation. The cost of manufacturing the extra colour-marker on the instrument is expected to be negligible in comparison to the price of the instrument itself. No special sterilization is needed. The system is very robust, both in the case of partial occlusion, and when the camera is very near to the instrument. Clinical experiments have demonstrated that the system can be reliably used for laparoscopic surgery. Automated laparoscope guidance promises to give back the surgeon his autonomy, particularly at standardised routine laparoscopic procedures as cholecystectomy fundoplication, hernia repair, or diagnostic laparoscopy.

5. Motion compensation of the beating heart

This section deals with motion compensation of the beating heart. The scenario and clinical background is introduced first, describing why beating heart surgery is beneficial for the

patient and why robotic systems are required to advance surgery in this field. Next, a region-based motion tracking scheme for the beating heart is described, with special focus on robustness of the approach. Finally, motion compensation is dealt with, before concluding with a summary and perspectives for future research.

5.1 Introduction

Tracking the motion of organs poses particular demands to the imaging system, since the target objects are deformable, as discussed above in section 2.3. This section starts with the stabilisation of organs and introduces the field of robotically assisted heart surgery thereafter.

5.1.1 Stabilisation of organs

While e.g. bone surgery allows for stereotactic fixation of the operating field, a complete stabilisation of the organ of interest is, in general, not possible in soft tissue sugery. The occurring motions are mainly due to respiration and heart beat, which is continued by the pulsating flow of blood in the vessels. Furthermore, organs are exposed to external forces during surgery, as e.g. when insufflating the abdomen with CC>2 during laparoscopic surgery or when tissue is drawn during surgery. These forces can cause the organs to change their position and to deform.

To perform surgery on the beating heart, a mechanical stabiliser is used to restrict motion in the operating field on the heart surface (Jansen, 1998). Since the heart tissue is elastic and deformable, this does not enable a complete fixation of the surface of the beating heart, however (Jacobs et al., 2003). The remaining motion is significant, especially for minimally invasive surgery at the beating heart, and a limiting factor to perform beating heart TECAB (totally endoscopic coronary artery bypass grafting, see below). The goal of the project described in the following is to compensate for this remaining motion of the beating heart.

5.1.2 Robot-assisted cardiac surgery

About three quarters of all annual heart surgeries in Germany (about 100 000) are bypass surgeries due to coronary heart diseases (800 000 cases worldwide) (Borst, 2001). During this kind of surgery the narrow part of a coronary vessel is bypassed with an healthy vessel, which is usually a vene from the leg or from the thoracic wall.

The conventional surgical technique brings along high strain for the patient, because the the thoracs is widely opened at the sternum to provide access the heart. To arrest the heart during the intervention the use of the heart-lung machine is necessary, in order to maintain the blood circulation. This brings along the danger of complications such as neurological disturbances by microembolies. Furthermore, the contact of blood with artificial surfaces can lead to general inflammation reactions. Also there are risks because of blood heparinisation to avoid thromboses. The overall high degree of traumatisation of the patient can lead to serious complications and accounts for a relatively high convalescence time of 2-3 months (Borst, 2001).

The high strain for the patient is approached to be reduced by two strategies:

On the one hand, surgery at the beating heart avoids the use of the heart-lung machine and thus also the risks that come with it. For beating heart surgery, the operating field is stabilised by a mechanical stabiliser, e.g. the Octopus™ system by Medtronic, which is fixed to the heart surface with small sucking mechanisms. (Jansen, 1998).

On the other hand, minimally invasive surgery avoids the highly traumatic sternotomy by using small incisions between the rips to access the heart. The surgical instruments and an

endoscopic camera are inserted through these so-called "ports". This surgical technique is known as TECAB (Totally Endoscopic Coronary Artery Bypass), and endoscopic robot systems are applied, with which the surgon controls the instruments inside the patient at an input console (cf. Fig. 6). The daVinci™system is an endoscopic surgerical robotic system which has been available for a few years (Guthart & Salisbury, 2000). The newly designed DLR surgical KineMedic robot (Ortmaier et al., 2006) will be able to to perform these tasks as well and adds a number of improvements (cf. section 3.4.
Minimally invasive surgery at the beating heart has been investigated at a few heart centres, such as Leipzig (heart centre, Prof. Dr. F. Mohr, PD Dr. V. Falk) (Mohr et al., 1999; Falk et al., 1999), Hamburg (University, Prof. Dr. H. Reichenspurner, PD Dr. D.H. Bohm, formerly in Munich-Grosshadern) (Reichenspurner et al., 1999b; Boehm et al., 1999), or in Canada (University of Western Ontario, Dr. W. Douglas Boyd) (Boyd et al., 2000).
Beating heart TECAB brings along considerable benefits for the patient, such that the convalescence time is reduced to a few days only. The surgical technique, however, poses strongly increased demands: In contrast to open surgery at the arrested heart, the contact to the operating field has to be established by a surgical robot system, the working space at the heart itself is very limited, and also the mechanically stabilised areas on the heart surface shows significant residual motions, which impede fast and safe interventions (Reichenspurner et al., 1999a; Jacobs et al., 2003).

5.1.3 Related work on motion compensation of the beating heart

The importance of motion compensation of the beating heart has been recognised and investigated in international research groups. Research has especially been performed by (Nakamura et al., 2001) and (Ginhoux et al., 2004). Both approaches, however, use artificial markers for motion estimation, which have to be fixed to the surface of the heart and the insertion and usage in the operating field of which brings along further difficulties. Therefore, using natural landmarks to estimate the motion of the beating heart ((Groger et al., 2002), section 5.3) is especially attractive. Moreover, region-based tracking of natural landmarks yields a particular texture unique for each landmark. This easily allows to track several landmarks concurrently, whereas using identical artifical landmarks bears the danger of ambiguities.

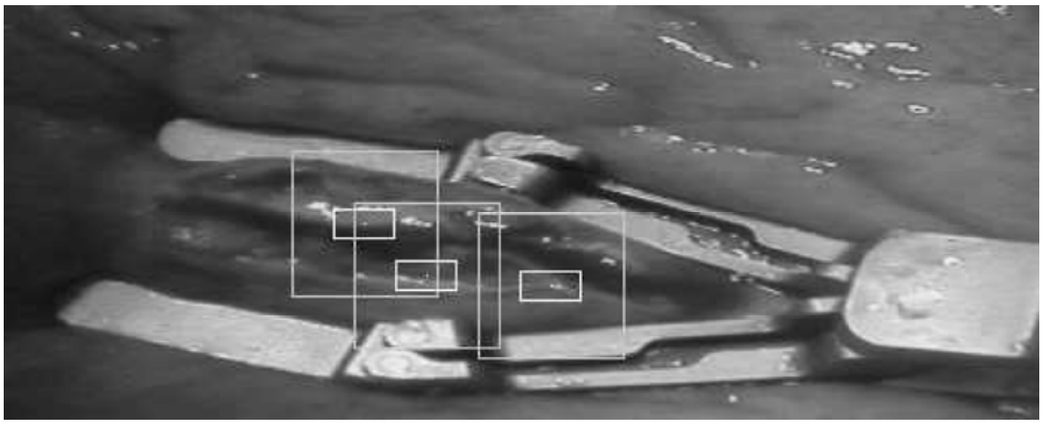

Figure 16. Mechnically stabilised heart with landmarks and tracking areas (from left to right LM2, LM8, and LM1)

Related work on motion compensation of the beating heart only allows for global correction of the image motion by moving the viewing camera according to motion captured (Nakamura et al., 2001; Ginhoux et al., 2004). However, as shown in (Groger & Hirzinger, 2006b), the motion of the beating heart cannot be fully reduced by compensating the occurring motion with a constant image correction factor.

5.2 Overview of the motion compensation scheme

Figure 17 gives a schematic overview of a possible solution for motion compensation in minimally invasive robotic surgery: The robot compensates the heart motion, such that the relative pose between the heart surface and the tool centre point of the surgical instrument remains constant (grey part of Fig. 17). The surgeon can then work on a virtually stabilised heart as he was used to in on-pump surgery, in which the heart does not move and the heart-lung machine is used to sustain the circulation. The following paragraphs describe this scheme in more detail.

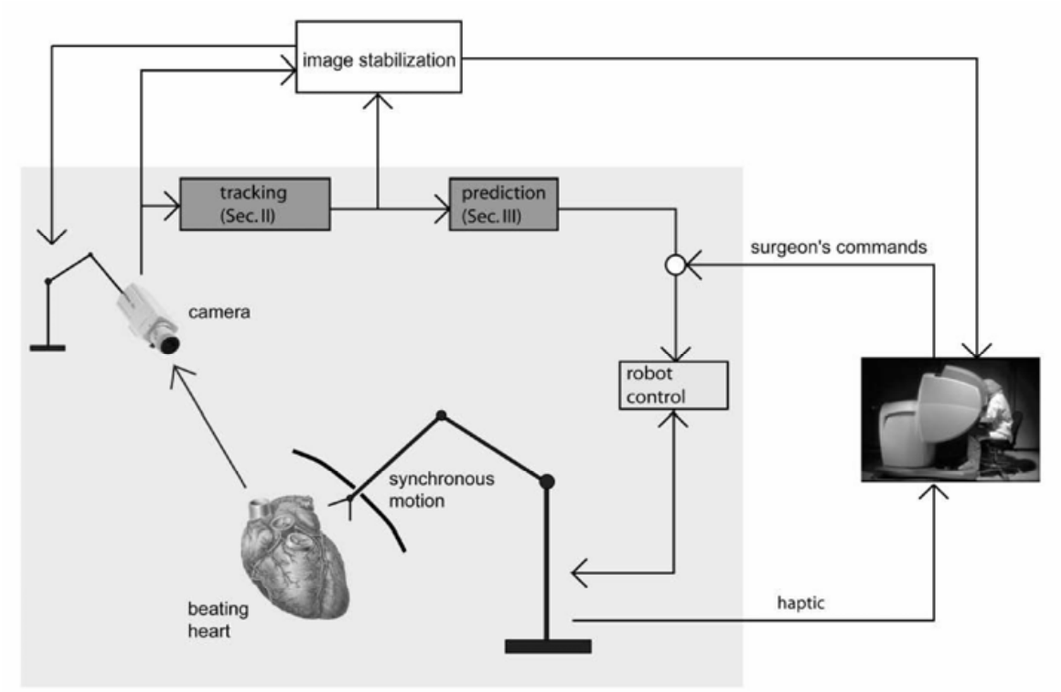

Figure 17. Schematic overview of motion compensation scheme

The surgeon's commands are superimposed on the motion of the instrument robot, which are calculated as shown in the inner part of Fig. 17. To perform the surgery it is not only necessary to move the surgical instruments according to the heart motion, but also to provide the surgeon with a stabilised image (see right part of Fig. 17 and (Falk et al., 1999)). Image stabilisation itself can be achieved either electronically by appropriate image warping algorithms or by moving the laparoscope robot in a way similar to the instrument robot, as indicated in the upper part of Fig. 17. Additionally, the surgeon can be provided with haptic (tactile or kinesthetic) feedback if appropriate surgical instruments at the slave side and displays at the master side are available (Kubler et al., 2005), (Preusche et al., 2001).

Before motion compensation in beating heart surgery can be performed, organ motion arising from the patient's respiration or heart beat has to be coped with. Therefore, the reliable measurement of this motion is an essential part of an advanced minimally invasive robotic surgery system (tracking block in the inner part of Fig. 17). Algorithms are presented which are able to track the motion of the 2-D projection of the beating heart surface by exploiting natural landmarks (see section 5.3). Motion tracking is made more robust by the prediction algorithms (inner part of Fig. 17) introduced in section 5.3.4, which are able to compensate for short failures of the motion estimation scheme. Furthermore, prediction is necessary to overcome the delays (data acquisition and processing, communication, etc.) which deteriorate the performance of the visual servoing control loop closed in the inner part of Fig. 17. Robust motion compensation (i.e. synchronous movement of heart surface and instrument, such that the relative distance /orientation between the instrument pose and selected frames lying on the heart surface remains almost constant) can be achieved only if these delays are eliminated. The robot control block is necessary for Cartesian control of the surgery robot as well as for taking the kinematic constraint at the entry point of the instrument into the human body into account. This is described in detail in (Ortmaier & Hirzinger, 2000) and will not be repeated here.

5.3 Motion tracking of the heart

Tracking the motion of the beating heart is the basic step for an approach to compensate the motion. This section introduces a region-based tracking strategy based on natural landmarks (Groger et al., 2002). After introducing the strategy, the issue of robust tracking is described and a few algorithms are presented to deal with this, such as the elimination of specular reflections and a multisensory prediction strategy.

5.3.1 Tracking model

As introduced in 2.1, region- and feature based tracking strategies can be distinguished. A region-based approach seems good for tracking landmarks on the heart surface, since all information should be used and geometric constraints on the tracking environment would be hard to establish. In the following, the model for tracking motion on the beating heart is introduced.

Parametric Model Given a reference pattern r, the task of tracking is to find the position of r in subsequent frames of an image sequence, or more generally, to find a transformation T mapping a pattern p in the current image to the original pattern r. The dissimilarity between two image patterns is expressed by the sum of squared differences (SSD) and is applied to determine suitable parameters of the transformation T:

$$J_{\mathrm{SSD}}(r,p) = \sum_{i \in \mathrm{dom}(r)} \left(r(i) - p(i)\right)^2, \tag{8}$$

where r and p are two image patterns and dom(r) denotes the domain of pattern r.

Searching for the best match of a reference pattern r in subsequent images, an image region p is allowed to be transformed according to the parameters of the model. The optimum motion parameter vector μ_{opt} minimising the dissimilarity between the reference and transformed patterns is given by

$$\mu_{\text{opt}} = \underset{\mu \in M}{\operatorname{argmin}} J_{\text{SSD}}(r, T_\mu(p)) \,, \tag{9}$$

where M is the set of all parameter vectors to the transformation T_μ, i.e. the search space to find μ_{opt}.

Affine Motion Model Although heart tissue is distorted nonlinearly, an affine motion model as in (Hager & Belhumeur, 1998) can be applied if the pattern is small enough to allow linear approximation. With the motion parameter vector μ, written as $\mu = (t_x, t_y, s, \phi, \tau, \alpha)^T$, the affine transformation i' of an image position vector $i = (i_x, i_y)^T$ is given by

$$i' \quad = \quad A \cdot i + t \,, \tag{10}$$

where $t = (t_x, t_y)^T$ is the translation vector, and the warping matrix A can be decomposed as

$$A \quad = \quad s \cdot \begin{pmatrix} \cos\phi & -\sin\phi \\ \sin\phi & \cos\phi \end{pmatrix} \cdot \begin{pmatrix} \cos\alpha & \sin\alpha \\ -\sin\alpha & \cos\alpha \end{pmatrix} \cdot \begin{pmatrix} 1 & 0 \\ 0 & \tau \end{pmatrix} \cdot \begin{pmatrix} \cos\alpha & -\sin\alpha \\ \sin\alpha & \cos\alpha \end{pmatrix} , \tag{11}$$

where s is the scaling parameter, ϕ the rotation angle, and τ and α are the shear parameter value and direction.

Illumination Model A linear compensation model is used to cope with illumination changes. It is applied to each pattern before the SSD measure is calculated to compare the reference and tracked patterns. Only mean compensation is demanded

$$\text{mean}(p) \quad \stackrel{\text{def}}{=} \quad \sum_{i \in \text{dom}(p)} p(i) \quad = \quad 0 \,, \tag{12}$$

which is achieved by shifting the intensities of a given pattern p such that their mean value is zero. Further compensation such as the normalisation of the standard deviation relating to the local contrast does not significantly improve tracking in the given heart images.

5.3.2 Elimination of specular reflections

The wet and glossy surface of the beating heart gives rise to frequent specular reflections of the light source, which disturb the tracking scheme considerably: These highlights are not bound to a particular surface structure and move according to the change in orientation between the light source and the heart surface. Strategies to detect the specular reflections and to reconstruct the underlying structure are developed and evaluated in (Groger et al., 2001, 2005): Structure inside specular areas is reconstructed using local structure information determined by the structure tensor, which provides a reliable measure of the orientation of structures. The reconstruction scheme uses intensity information mainly from boundary pixels along the current local orientation and interpolates linearly between these intensities. Thus, surface structure in the image is continued and smooth transitions at the boundaries are ensured. Preprocessing endoscopic heart images by this scheme makes the subsequent tracking considerably more robust toward specular reflections (Groger et al., 2001). The results given below are based on video sequences processed in this way.

5.3.3 Motion trajectories

Investigations show that the affine motion model described by Eq. 10 can be simplified from six to two degrees of freedom (i.e. a two-dimensional translation vector) to capture the heart motion

in the stabilised area (Groger et al., 2002). To determine the significance of the parameters of the motion model, the parameter space is searched exhaustively to find the best match.
The quality of tracking and the appropriateness of the suggested tracking model is shown by an analysis of the trajectories of the parameters associated with the tracked pattern. This analysis assesses the occurrence of outliers from the expected trajectory and the strength of the signal indicated by the appearance of dominant frequency components in the amplitude spectrum of the trajectory. Outlier measures developed in (Groger et al., 2002) calculate the total number of outliers and the distance of a given trajectory from its smooth version.

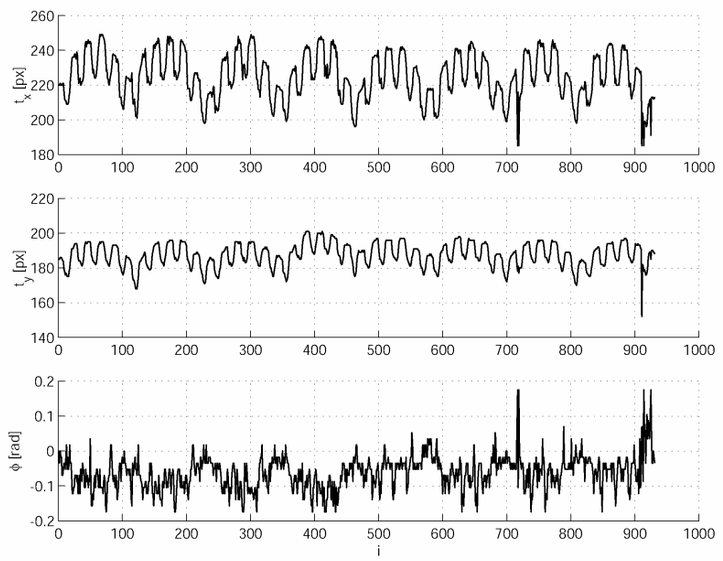

Figure 18. Selected trajectories of the affine parameters of landmark LM2. The temporal resolution is 40 ms (25 Hz frame rate). Translation in x and y are given in pixel [px], rotation ϕ in radians [rad]

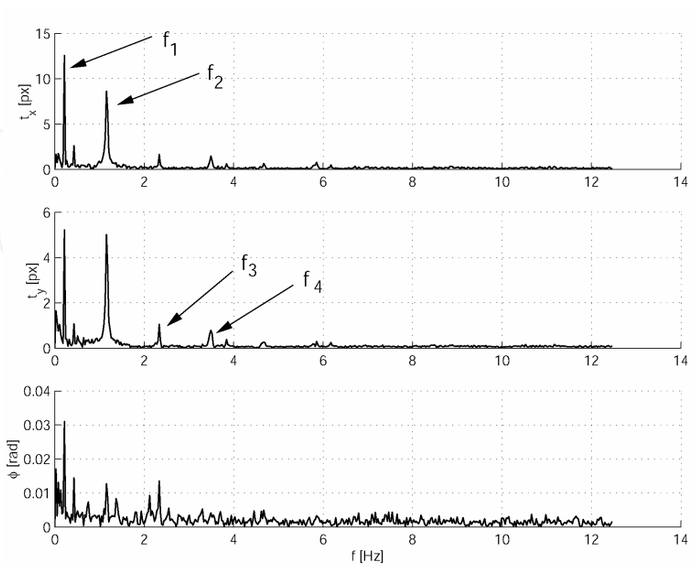

Figure 19. Amplitude spectrum of selected affine parameters at landmark LM2

The quasi-periodic progression of the translational parameters is presented in Fig. 18. The other parameters are strongly disturbed and thus hardly contain any useful information (see Fig. 18 for the rotational parameter ϕ. Reduction of dimensions of the parameter search space to only two translational degrees of freedom allows to efficiently obtain the optimum $\mu_{\text{opt}} \in M$ (section 5.3.1, Eq. 9. Moreover, this enables realtime implementation on a standard computer with simultaneous tracking of several landmarks as in section 5.3.4. The small search space allows for exhaustive search for μ_{opt} in realtime, thus avoiding errors by local minima.
The results presented here are confirmed by details given in (Groger et al., 2002). Tracking of e.g. 332 equally distant landmarks over 931 frames in the stabilised area of Fig. 16 with the proposed translational tracking model shows that more than 97% of all positions and frames are tracked without outliers.
The amplitude spectrum of the translation parameters shows two dominant peaks at f_1 = 0.24 Hz and f_2 = 1.18 Hz (see Fig. 19). The frequency f_1 corresponds to the respiration rate of the patient, f_2 to the heart rate. The influence of respiration on the measured heart motion becomes clear if the patient anatomy is considered. The respiration effect causes the diaphragm moving up and down, which yields an additional motion superimposed to the motion caused by the heart beat itself. The distribution of the dominant peaks depends on the current setup, e.g. the image coordinate system or the placement of the mechanical stabiliser. In addition to f_1 and f_2, the first and second harmonics of the (non-sinusoidal) heart beat can be extracted from the amplitude spectrum: f_3 = 2.36 Hz and f_4 = 3.54 Hz. The amplitude spectrum of the rotational parameter shows similar behaviour, but the dominant frequencies are much less pronounced.
The spectrum analysis shows that the trajectories of tracked positions are strongly correlated with heart beat and respiration. Since the amplitude spectrum only provides a global view of the trajectory, natural changes of the physiological parameters are not taken into account. Therefore, the spectrum is only used to show the correctness of the applied tracking model but not considered in the proposed motion tracking scheme.

5.3.4 Motion prediction

The motion parameters of a mechanically stabilised beating heart can be captured by exploiting natural landmarks as shown before. Nevertheless, landmarks may be occluded for a short time (e.g., by surgical instruments) and cause tracking to fail. To guarantee robust motion parameter estimation under these circumstances, algorithms were developed which are able to predict these parameters if no tracking information is available. This will not only bridge missing tracking information, but also allow dynamic positioning of the tracking search area. Additionally, prediction is useful for motion compensation: it helps to overcome the delay time of the closed controller loop (including video capturing, data processing, and data transmission) and, thus, increases the bandwidth of the robotic system and, therefore, improves the quality of motion compensation.
As illustrated in Fig. 20, if tracking information is not available, the prediction scheme estimates the expected position of a given landmark from its past trajectory. Therefore, the best matching "embedding" vector is calculated (for more detail see (Ortmaier et al., 2002), (Ortmaier et al., 2005)).
This enables to predict the motion of a landmarks with high accuracy over a number of frames. The extension of the prediction approach to multiple landmarks (Ortmaier et al., 2005) also takes the trajectories of the remaining landmarks into account. Thus, motion can

be predicted for a longer period, as is the case with short-time occlusion by an instrument. To increase robustness of motion estimation even more, and to account for larger occlusions as well, which several landmarks can be concerned of, additional sensor signals such as the respiration pressure signal and the ECG of the patient contribute to a multisensory prediction strategy (Ortmaier et al., 2005).

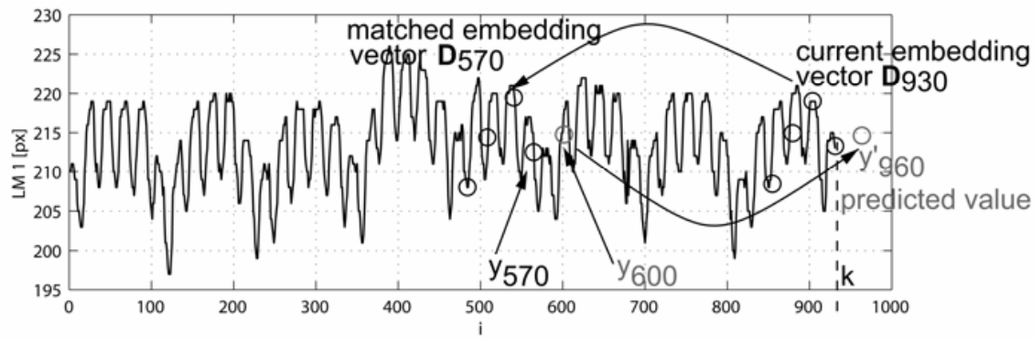

Figure 20. Illustration of the local prediction scheme

5.4 Motion compensation of the heart

As introduced in section 5.2, the motion compensation of the beating heart requires a robotic system, capable of both sufficient accuracy and dynamics to follow the motion of the beating heart. As one possible strategy the robot can move the endoscope to stabilise the motion of the beating heart in a global stabilisation approach. However, since the motion of the heart surface varies locally, this method is not sufficient to fully stabilise the motion of the heart surface as shown in (Groger & Hirzinger, 2006b). Another strategy is to compensate heart motion digitally, i.e. by stabilising the image presented to the surgeon. A special approach to achieve this is presented in (Groger & Hirzinger, 2006a). It is based on robust motion estimation of natural landmarks on the heart surface and uses an efficient interpolation strategy to build dense field of motion correction for the image. Results show that the image motion can be significantly reduced by this approach (Groger & Hirzinger, 2006a). The degree of image motion correction has to be performed in accordance to motion compensation of the surgical instrument, which requires the system to maintain a high degree of consistency in the motion compensation strategy.

Further investigations will involve the the new KineMedic robot (Ortmaier et al., 2006), which provides a considerably higher degree of accuracy and dynamics than existing medical robotic systems, which is required for the task of motion compensation of the beating heart.

6. Conclusion

Motion tracking in minimally invasive surgery is a fundamental issue to adapt medical robotic systems to the changing environment of the operating field. The two example scenarios show that the intelligent and adaptive robotic systems can contribute considerably to make surgery more gentle to the patient by reducing traum and to assist the surgeon with the increased demands and difficulaties of minimally invasive surgery, in which direct contact is lost to the operating field.

Automated laparoscope guidance fulfills the assistant surgeon's task of camera guidance in a reliable and non-exhausting manner, and represents an important step towards minimally

invasive solo surgery. Motion compensation of the beating heart is a key step towards beating heart TECAB, a cardiac surgical technique, which is most beneficial to the patient. Further investigations of the described projects involve the newly developed DLR KineMedic robotic system.

7. Acknowledgements

In particular, the authors would like to thank the clinical projects partners: Prof. Dr. H. Feussner from the Department of Surgery at the Klinikum rechts der Isar (MRIC) of the Technical University of Munich contributed the medical part to the automated laparoscopic guidance project. PD Dr. D.H. Bohm from the Department of Cardiovascular Surgery at the University Hospital of Hamburg-Eppendorf (UKE), Germany, is the clinical partner for the project on motion compensation of the beating heart.

8. References

Arbter, K. & Kish, D. (2004). Bin Entwurfswerkzeug fur Farbklassifikatoren in Echtzeitanwendungen, in: *10. Workshop Farbbildverarbeitung,* Koblenz, Germany

Arbter, K. & Wei, G.Q. (1996). Verfahren zum Nachfuhren eines Stereo-laparoskopes in der minimal invasiven Chirurgie, German patent no. 19529950

Arbter, K. & Wei, G.Q. (1998). Method of tracking a surgical instrument with a mono or stereo laparoscope, US patent no. 5820545

Bardinet, E.; Cohen, L. & Ayache, N. (1996). Tracking medical 3D data with a deformable parametric model, in: *Proc. European* Con/. *Computer Vision,* vol. 1, pp. 317-328

Bargar, W.; Bauer, A. & Borner, M. (1998). Primary and revision - total hip replacement using the robodoc system, *Clinical Orthopaedics and Related Research,* vol. 354:pp. 82-91

Black, M. & Yacoob, Y. (1995). Tracking and recognizing rigid and non-rigid facial motions using local parametric models of image motion, in: *International Conference on Computer Vision (ICCV),* pp. 374-381

Boehm, D.H.; Reichenspurner, R.; Gulbins, H.; Detter, C.; Meiser, B.; Brenner, P.; Habazettl, H. & Reichart, B. (1999). Early experience with robotic technology for coronary artery surgery, *Annals of Thoracic Surgery,* vol. 68:pp. 1542-1546

Borst, C. (2001). Operieren am schlagenden Herz, *Spektrum der Wissenschaft,* pp. 50-55

Boyd, W.; Rayman, R. & Desai et al., N. (2000). Closed-chest coronary artery bypass grafting on the beating heart with the use of a computer-enhanced surgical robotic system, *J Thorac Cardiovasc Surg,* vol. 120:pp. 807-809

Casals, A.; Amat, J.; Prats, D. & Laporte, E. (1995). Vision guided robotic system for laparoscopic surgery, in: *Proc. 7th Int.* Con/, *in Advanced Robotics, ICAR'95,* pp. 33-36, Sant Feliu de Guixols-Spain

Computer Motion Inc., 130-B Cremona Drive, G.C..U. (1994). AesoplOOO users guide

Corke, P. (1993). Visual control of robot manipulators - a review, in: K. Hashimoto (Ed.), *Visual Servoing,* pp. 1-31, World Scientific

Doignon, C.; Nageotte, F. & de Mathelin, M. (2004). Detection of grey regions in color images: application to the segmentation of a surgical instrument in robotized laparoscopy, in: *Proceedings of the IEEE/RSJ International Conference on Intelligent Robots and Systems,* pp. 3394-3399, Sendai, Japan

Doignon, C.; Nageotte, F. & de Mathelin, M. (2006). Segmentation and guidance of multiple rigid objects for intra-operative endoscopic vision, in: *International Workshop on Dynamical Vision, in conjunction with ECCV 2006,* Springer, Graz, Austria

Falk, V; Diegeler, A.; Walther, T.; Loscher, N.; Vogel, B.; Ulmann, C.; Rauch, T. & Mohr, F.W. (1999). Endoscopic coronary artery bypass grafting on the beating heart using a computer enhanced telemanipulation system, *Heart Surg Forum,* vol. 2:pp. 199-205

Foley, J.; van Dam, A.; Feiner, S. & Hughes, J. (1990). *Computer Graphics: Principles and Practice,* 2nd ed., Addison-Wesley, Reading, Massachusetts

Ginhoux, R.; Gangloff, J.; de Mathelin, M.; Soler, L.; Sanchez, M.A. & Marescaux, J. (2004). Beating heart tracking in robotic surgery using 500 Hz visual servoing, model predictive control and an adaptive observer, in: IEEE *International Conference on Robotics and Automation (ICRA),* pp. 274-279, New Orleans, USA

Groger, M. & Hirzinger, G. (2006a). Image stabilisation of the beating heart by local linear interpolation, in: K. Cleary & R. Galloway (Eds.), *Medical Imaging 2006: Visualization, Image-Guided Procedures, and Display,* vol. 6141 of *Proceedings ofSPIE,* San Diego, USA

Groger, M. & Hirzinger, G. (2006b). Optical flow to analyse stabilised images of the beating heart, in: A. Ran-chordas; H. Araujo & B. Encarnacao (Eds.), *International Conference on Computer Vision Theory and Applications (VISAPP),* pp. 237-244, INSTICC Press, Setubal, Portugal

Groger, M.; Sepp, W; Ortmaier, T. & Hirzinger, G. (2001). Reconstruction of image structure in presence of specular reflections, in: B. Radig & S. Florczyk (Eds.), *Pattern Recognition, Proc. 23rd DAGM Symposium,* vol. 2191 of *LNCS,* pp. 53-60, Springer, Munich, Germany

Groger, M.; Ortmaier, T.; Sepp, W. & Hirzinger, G. (2002). Tracking local motion on the beating heart, in: S.K. Mun (Ed.), *Medical Imaging 2002: Visualization, Image-Guided Procedures, and Display,* vol. 4681 of *Proceedings ofSPIE,* pp. 233-241, San Diego, USA

Groger, M.; Sepp, W. & Hirzinger, G. (2005). Structure driven substitution of specular reflections for realtime heart surface tracking, in: IEEE *International Conference on Image Processing (ICIP),* vol. 2, pp. 1066-1069, Geneva, Italy

Guthart, G. & Salisbury, J. (2000). The Intuitive telesurgery system: Overview and application, in: IEEE *International Conference on Robotics and Automation (ICRA),* pp. 618-621, San Francisco, USA

Hager, G. (1997). A modular system for robust hand-eye coordination using feedback from stereo vision, IEEE *Transactions on Robotics and Automation,* vol. 13(4):pp. 582-595

Hager, G. & Belhumeur, P. (1998). Efficient region tracking with parametric models of geometry and illumination, IEEE *Transactions on Pattern Analysis and Machine Intelligence,* vol. 20(10)

Hirzinger, G.; Albu-Schaffer, A.; Hahnle, M.; Schafer, I. & Sporer, N. (2001). A new generation of torque controlled light-weight robots, in: IEEE *International conference on Robotics and Automation (ICRA),* pp. 3356-3363, Seoul, Korea

Hurteau, R.; DeSantios, S.; Begin, E. & Gagner, M. (1994). Laparoscopic surgery assisted by a robotic cameraman: Concept and experimental results, in: *Proc. IEEE Int.* Con/. *Robotics and Automation (ICRA),* pp. 2286-2289, San Diego

Hutchinson, S.; Hager, G. & Corke, P. (1996). A tutorial introduction to visual servo control, IEEE *Transactions on Robotics and Automation,* vol. 12(5):pp. 651-670

Jacobs, S.; Holzhey, D.; Kiaii, B.; Onnasch, J.; Walther, T.; Mohr, F. & Falk, V (2003). Limitations for manual and telemanipulator-assisted motion tracking - implications for endoscopic beating-heart surgery, *Ann Thome Surg,* vol. 76:pp. 2029-2035

Jansen, E. (1998). *Towards minimally invasive coronary arterry bypass grafting,* Brouwer Uithof, Utrecht Kazanzides, P.; Mittelstadt, B.; Musits, B.L.; Bargar, W.L.; Zuhars, J. & et al. (1995). An integrated system for cementless hip replacement, IEEE *Eng. Med. Biol. Mag.,* vol. 14:pp. 307-313

Kiibler, B.; Seibold, U. & Hirzinger, G. (2005). Development of acutated and sensor integrated forceps for minimally invasive robotic surgery, *International Journal of Medical Robotics and Computer Assisted Surgery,* vol. l(3):pp. 96-107

Lee, C; Wang, Y.; Uecker, D. & Wang, Y. (1994). Image analysis for automated tracking in robot-assisted endoscopic surgery, in: *Proc. Int.* Con/. *Pattern Recognition,* pp. A:88-92

Mclnerney, T. & Terzopoulos, D. (1995). A dynamic finite element surface model for segmentation and tracking in multidimensional medical images with application to cardiac 4d image analysis, *Computerized Medical Imaging and Graphics,* vol. 19(l):pp. 69-83

Mclnerney, T. & Terzopoulos, D. (1996). Deformable models in medical image analysis: A survey, *Medical Image Analysis,* vol. l(2):pp. 91-108

Mittelstadt, B.; Kazanzides, P.; Zuhars, J.; Williamson, B.; Cain, P.; Smith, F. & Bargar, W. (1996). *Computer-Integrated Surgery,* chap. The evolution of a surgical robot from prototype to human clinical use, pp. 397-407, MIT Press, Cambridge, MA

Mohr, F.W.; Falk, V.; Diegeler, A. & Autschbach, R. (1999). Computer enhanced coronary artery bypass surgery, / *Thorac Cardiovasc Surg,* vol. 117:pp. 1212-1213

Moran, M. (1993). Stationary and automated laparoscopically assisted technologies, *Journal of Laparoendoscopic Surgery,* vol. 3(3):pp. 221-227

Nakamura, Y; Kishi, K. & Kawakami, H. (2001). Heartbeat synchronization for robotic cardiac surgery, in: IEEE *International Conference on Robotics and Automation (ICRA),* pp. 2014-2019, Seoul, Korea

Omote, K.; Feussner, H.; Ungeheuer, A.; Arbter, K.; Wei, G.Q.; Siewert, J.R. & Hirzinger, G. (1999). Self-guided robotic camera control for laparoscopic surgery compared with human camera control, *The American Journal of Surgery,* vol. 117:pp. 321-324 Ortmaier, T. &

Hirzinger, G. (2000). Cartesian control issues for minimally invasive robot surgery, in: IEEE *Int. Conference on Intelligent Robots and Systems (IROS),* Takamatsu, Japan

Ortmaier, T.; Reintsema, D.; Seibold, U.; Hagn, U. & Hirzinger, G. (2001). The DLR minimally invasive robotics surgery scenario, in: G. Fa'rber & J. Hoogen (Eds.), *Workshop on Advances in Interactive Multimodal Telepresence Systems,* pp. 135-147, Munich, Germany

Ortmaier, T.; Groger, M. & Hirzinger, G. (2002). Robust motion estimation in robotic surgery on the beating heart, in: *Computer Assisted Radiology and Surgery (CARS),* pp. 206-211, Paris, France

Ortmaier, T.; Groger, M.; Boehm, D.; Falk, V. & Hirzinger, G. (2005). Motion estimation in beating heart surgery, IEEE *Transactions on Biomedical Engineering (TBME),* vol. 52(10):pp. 1729-1740

Ortmaier, T.; Weiss, H.; Hagn, U.; Grebenstein, M.; Nickl, M.; A. Albu-Schaffer, C. Ott, S.J.; Konietschke, R.; Le-Tien, L. & Hirzinger, G. (2006). A hands-on-robot for accurate placement of pedicle screws, in: IEEE *International Conference on Robotics and Automation (ICRA),* pp. 4179-4186, Orlando, USA

Preusche, C.; Ortmaier, T. & Hirzinger, G. (2001). Teleoperation Concepts in Minimal Invasive Surgery, in: *Proceedings of 1st IFAC Conference on Telematics Application in Automation and Robotics,* VDI/VDE - GMA, Weingarten, Germany

Reichenspurner, H.; Boehm, D.H.; Welz, A.; Schulze, C.; Gulbins, H. & Wildhirt, S. (1999a). 3D-Video- and robot-assisted port access mitralvalve surgery, *Annals of Thoracic Surgery*

Reichenspurner, H.; Damiano, R.; Mack, M.; Boehm, D.H.; Gulbins, H.; Meiser, B.; Elgafi, R. & Reichhart, B. (1999b). Experimental and first clinical use of the voice-controlled and computer-assisted surgical system ZEUS for endoscopic coronary artery bypass grafting, *Journal of Thoracic and Cardiovascular Surgery,* vol. 118:pp. 11-16

Sackier, J. & Wang, Y. (1996). *Computer-Integrated Surgery,* chap. Robotically Assisted Laparoscopic Surgery: From Concept to Development, pp. 577-580, MIT Press, Cambridge, MA, USA

Shi, J. & Tomasi, C. (1994). Good features to track, IEEE *Conference on Computer Vision and Pattern Recognition,* pp.593-600

Taylor, R.; Paul, H.; Mittelstadt, B. & et al. (1989). A robotic system for cementless total hip replacement surgery in dogs, in: *Proc. 2nd Workshop Medical and Healthcare Robotics,* Newcastle-on-Tyne, U. K.

Taylor, R.; Funda, J.; Eldridge, B.; Gomory, S.; Gruben, K. & et. al (1995). A telerobotic assistant for laparoscopic surgery, IEEE *Engineering in Medicine and Biology,* vol. 14:pp. 279-288

Taylor, R.H.; Paul, H.; Kazandzides, P.; Mittelstadt, B.; Hanson, W; Zuhars, J.; B.Williamson; Musits, B.; Glassman, E. & Bargar, W. (1994). An image-directed robotic system for precise orthopaedic surgery, IEEE *Trans. Robot. Automat.,* vol. 10:pp. 261-275

Taylor, R. & Stoianovici, D. (2003). Medical robotics in compter-integrated surgery, IEEE *Transactions on Robotics and Automation,* vol. 19(5):pp. 765-781

Tonet, O.; Thoranaghatte, R.; Megali, G. & Dario, P. (2007). Tracking endoscopic instruments without a localizer: A shape-analysis-based approach, *Computer Aided Surgery,* vol. 12(l):pp. 35-42

Troccaz, J. (1994). Robots in surgery, in: *Proc. Int. Symposium on Robotics Research,* Herrsching, Germany Turner, D. (1995). Solo surgery with aid of a robotic assistant, in: *Proc. Int.* Con/. *Telemedicine and Telecare,* pp. 83-86, London, U.K.

Ungeheuer, A.; Arbter, K.; Omote, K.; Feussner, H.; Wei, G.Q.; Siewert, J.R. & Hirzinger, G. (1997). Selbststeuernde farbcodierte Kamerafiihrung bei laparoskopischen Eingriffen, *Minimal invasive Chirurgie,* vol. 6.3:pp. 41-47

Voros, S.; Orvain, E.; Cinquin, P. & Long, J.A. (2006). Automatic detection of instruments in laparoscopic images: a first step towards high level command of robotized endoscopic holders, in: *First IEEE/RAS- EMBS International Conference on Biomedical Robotics and Biomechatronics (BioRob)*

Wei, G.Q.; Arbter, K. & Hirzinger, G. (1997). Real-time visual servoing for laparoscopic surgery, IEEE *Engineering in Medicine and Biology,* vol. 16(l):pp. 40-45

Wintermantel, E. & Ha, S.W (Eds.) (2001). *Biokompatible Werkstoffe fur die therapeutische Medizintechnik,* Springer Verlag

Y. S. Kwoh, J.H. & et al., E.A.J. (1988). A robot with improved absolute positioning accuracy for ct-guided stereotactic brain surgery, IEEE *Trans. Biomed. Eng.,* vol. 35:pp. 153-161

Medical Robotics

Edited by Vanja Bozovic

ISBN 978-3-902613-18-9
Hard cover, 526 pages
Publisher I-Tech Education and Publishing
Published online 01, January, 2008
Published in print edition January, 2008

The first generation of surgical robots are already being installed in a number of operating rooms around the world. Robotics is being introduced to medicine because it allows for unprecedented control and precision of surgical instruments in minimally invasive procedures. So far, robots have been used to position an endoscope, perform gallbladder surgery and correct gastroesophogeal reflux and heartburn. The ultimate goal of the robotic surgery field is to design a robot that can be used to perform closed-chest, beating-heart surgery. The use of robotics in surgery will expand over the next decades without any doubt. Minimally Invasive Surgery (MIS) is a revolutionary approach in surgery. In MIS, the operation is performed with instruments and viewing equipment inserted into the body through small incisions created by the surgeon, in contrast to open surgery with large incisions. This minimizes surgical trauma and damage to healthy tissue, resulting in shorter patient recovery time. The aim of this book is to provide an overview of the state-of-art, to present new ideas, original results and practical experiences in this expanding area. Nevertheless, many chapters in the book concern advanced research on this growing area. The book provides critical analysis of clinical trials, assessment of the benefits and risks of the application of these technologies. This book is certainly a small sample of the research activity on Medical Robotics going on around the globe as you read it, but it surely covers a good deal of what has been done in the field recently, and as such it works as a valuable source for researchers interested in the involved subjects, whether they are currently “medical roboticists” or not.

INTECH
open science | open minds

InTech Europe
University Campus STeP Ri
Slavka Krautzeka 83/A
51000 Rijeka, Croatia
Phone: +385 (51) 770 447

InTech China
Unit 405, Office Block, Hotel Equatorial Shanghai
No.65, Yan An Road (West), Shanghai, 200040, China
中国上海市延安西路65号上海国际贵都大饭店办公楼405单元
Phone: +86-21-62489820

Fax: +385 (51) 686 166
www.intechopen.com

Fax: +86-21-62489821

IntechOpen